Am J Physiol Heart Circ Physiol 283: H1116–H1122, 2002;
10.1152/ajpheart.00927.2001.

Increased vulnerability to inducible atrial fibrillation caused by partial cellular uncoupling with heptanol

TOSHIHIKO OHARA, ZHILIN QU, MOON-HYOUNG LEE, KEIKO OHARA, CHIKAYA OMICHI, WILLIAM J. MANDEL, PENG-SHENG CHEN, AND HRAYR S. KARAGUEUZIAN
Division of Cardiology, Cedars-Sinai Research Institute, Department of Medicine, University of California of Los Angeles School of Medicine, Los Angeles, California 90048

Received 25 October 2001; accepted in final form 22 May 2002

Ohara, Toshihiko, Zhilin Qu, Moon-Hyoung Lee, Keiko Ohara, Chikaya Omichi, William J. Mandel, Peng-Sheng Chen, and Hrayr S. Karagueuzian. Increased vulnerability to inducible atrial fibrillation caused by partial cellular uncoupling with heptanol. *Am J Physiol Heart Circ Physiol* 283: H1116–H1122, 2002; 10.1152/ajpheart.00927.2001.—We hypothesized that partial cellular uncoupling produced by low concentrations of heptanol increases the vulnerability to inducible atrial fibrillation (AF). The epicardial surface of 12 isolated-perfused canine left atria was optically mapped before and after 1–50 μM heptanol infusion. At baseline, no sustained (>30 s) AF could be induced in any of the 12 tissues. However, after 2 μM heptanol infusion, sustained AF was induced in 9 of 12 tissues ($P < 0.001$). Heptanol >5 μM caused loss of 1:1 capture during rapid pacing, causing no AF to be induced. AF was initiated by conduction block across the fiber leading to reentry, which broke up after one to two rotations into two to four independent wavelets that sustained the AF. Heptanol at 2 μM had no effect on the cellular action potential duration restitution or on the maximal velocity rate over time of the upstroke. The effects of heptanol were reversible. We conclude that partial cellular uncoupling by heptanol without changing atrial active membrane properties promotes wavebreak, reentry, and AF during rapid pacing.

optical mapping; reentry

CONDUCTION VELOCITY (CV) and safety of wave-front propagation depend on both the active membrane properties of each cell of the conducting pathway and of the cell-to-cell gap junctional conductance (coupling) (13, 24). The importance of junctional conductance in altering conduction and promoting conduction block and ventricular arrhythmias was emphasized in experimental (2, 4, 11, 13, 24) and simulation (12, 13, 22) studies. Recent studies (8) using transgenic mice with gap junctional connexin40 (Cx40) deficiency showed that burst atrial pacing in these mice can induce atrial conduction disturbances and atrial tachyarrhythmia. At present, the roles of selective and partial atrial gap junctional uncoupling in inducing atrial tachycardia (AT) and atrial fibrillation (AF) in larger animals remain poorly explored. It has been suggested that aging might be associated with increased cellular uncoupling (24), a phenomenon that might contribute to the increased incidence of AF in the elderly (3). We hypothesized that partial cellular uncoupling produced by heptanol at concentrations that do not alter the active membrane properties promotes wave break of the activation wave front during rapid pacing, leading to AF.

METHODS AND MATERIALS

Isolated left atrial tissue preparation. The research protocol was approved by the Institutional Animal Care and Use Committee of Cedars-Sinai Medical Center and followed the guidelines of the American Heart Association. Twelve mongrel dogs of either sex weighing between 22 and 28 kg were anesthetized with intravenous pentobarbital sodium (35 mg/kg). The left atrium (LA) was isolated, cannulated, and perfused at a flow rate of 15 ml/min with 37°C oxygenated Tyrode solution as described previously (31). Two pairs of bipolar electrodes (one for pacing and one for recording) were placed 1.5–2 cm apart. In addition, two electrodes were placed at the edges of the tissue 4 cm apart from each other to record global atrial rhythm ("pseudoelectrocardiogram") (31).

Test of AF vulnerability: effects of heptanol. Development of conduction disturbances and changes in the vulnerability to AF were tested by rapid atrial pacing at 50 ms cycle length (CL) for 3 s by using 5-ms pulses of twice diastolic current threshold. Five attempts of AF induction were tested at baseline in each of the 12 isolated tissues (60 trials), and five attempts were tested after 2 μM heptanol infusion (60 trials). Because AF could be induced only with 2 μM heptanol (see RESULTS), the effects of 1, 5, 10, and 50 μM heptanol were tested in only five tissues. If the induced AF was sustained for >5 min, it was cardioverted with an external defibrillator (HVS-02, Ventritex). During rapid pacing at 50 ms CL, the mean shortest captured CL was determined before and after heptanol perfusion with a pair of recording bipolar electrodes located 1–2 cm away from the pacing electrode. Reversibility of the the effects of heptanol was evaluated after 30 min of drug-free Tyrode solution perfusion ($n = 6$).

Optical mapping. Wave-front dynamics during pacing and AF were analyzed using an optical mapping system. The LA was stained for 20 min with di-4-ANEPPS (10 μM). The patterns of activation were acquired with a charge-coupled device (CCD) camera with a sampling interval of 2.3 ms for a

Address for reprint requests and other correspondence: H. S. Karagueuzian, Cedars-Sinai Medical Center, Davis Research Bldg. Rm. 6066, 8700 Beverly Blvd., Los Angeles, CA 90048 (E-mail: karagueuzian@cshs.org).

The costs of publication of this article were defrayed in part by the payment of page charges. The article must therefore be hereby marked "*advertisement*" in accordance with 18 U.S.C. Section 1734 solely to indicate this fact.

duration of 2.3 s in a recording field of ~28 by 28 mm with 128 by 128 pixel resolution. The optical mapping system is similar to the one described previously (18, 19). A solid laser with a wavelength of 532 nm was used for the light source, and the induced fluorescence was collected with 12-bit digital CCD camera. The fluorescent signals were baseline subtracted and inverted. The signals of each pixel were then spatially averaged with the signals of eight neighboring pixels to reduce noise. The computer first finds every adjacent pair of pixels in the frame that cross the average value of the data. If the intensity of the data on which the line coincides is increasing, that edge is identified as the wave front and is colored red. The color then progressively changes to yellow, green, light blue, and finally dark blue to represent increasing states of repolarization (Fig. 1). Isochronal activation maps were also constructed during pacing before and after heptanol exposure (26).

We define development of wave break in a propagating wave front as a point along the front where the activation wave front and the repolarization wave back meet. Wave break (wave splitting) is defined as the generation of two daughter wavelets from a single wave front. The sites of block during pacing and during AF were determined and then related to the underlying atrial fiber orientation. The presence of multiple independent wave fronts during AF was ascertained by the presence of repolarized tissue between the wave fronts and by the different directions of propagation of the wave front.

Conduction velocity. CV was measured over the left epicardial appendage along the fiber during atrial pacing at different pacing CLs (PCLs, 600–200 ms) and during AF. The CV during pacing was calculated as the ratio of the distance traveled by the wave front to the time it took to travel between the pacing and the recording electrodes, which were 1.5–2 cm apart from each other (5). The CV during AF was determined by the ratio of the distance traveled continuously by the wave front to the time it took to travel the distance (i.e., 0.5 cm to 1.5 cm).

Transmembrane action potential recording. Transmembrane action potential (TMPs) were recorded with glass microelectrodes from the superficial cell layers (2–4 cells deep) of the epicardium of the LA free wall. The TMP data were

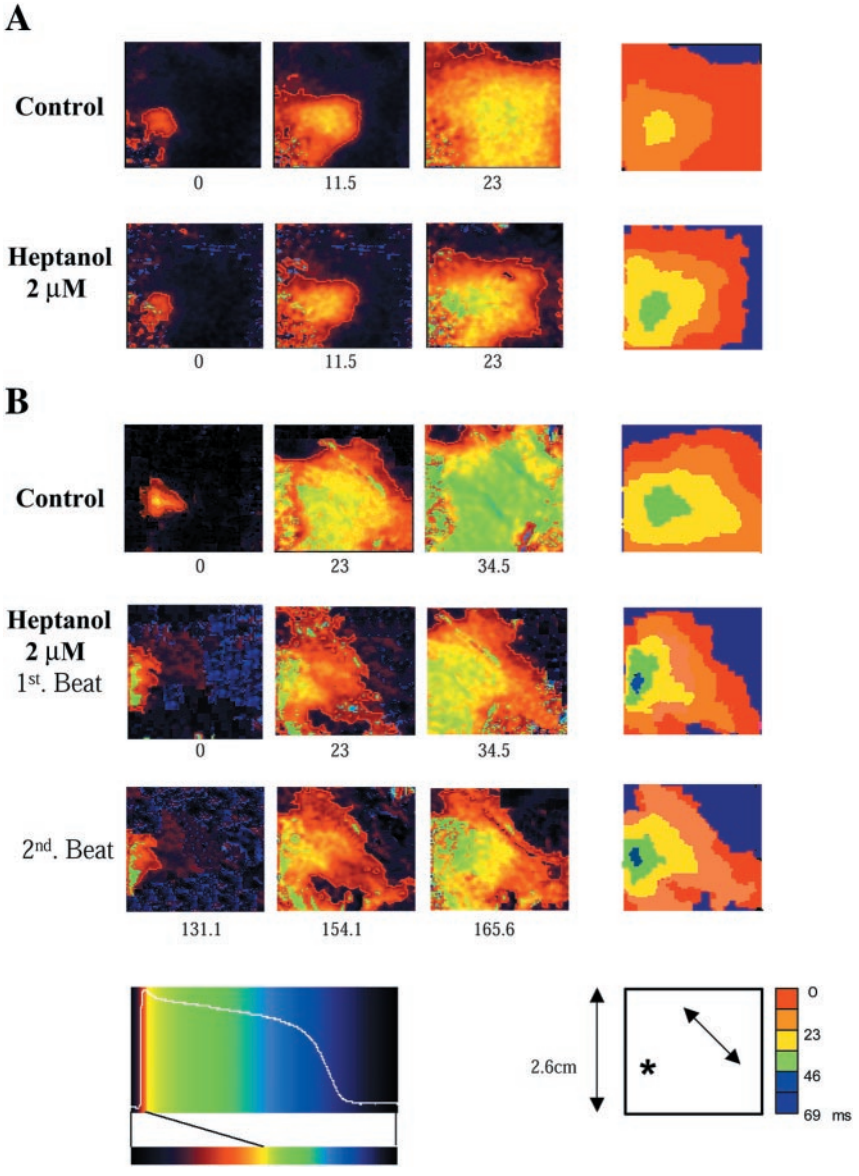

Fig. 1. Snapshots and isochronal optical mapping before (Control) and after heptanol (2 μM) during 400- (*A*) and 130-ms (*B*) pacing cycle lengths (PCL) in an isolated canine left atrium. Heptanol causes conduction slowing at 400-ms PCL and conduction block across the fiber during 130-ms PCL (second paced beat). *Bottom left* and *right* show the color code for the snap shots (first 3 frames in each row) and isochronal maps (last frames in each row). Double-headed arrow shows the fiber orientation. *Pacing site. Number under each snapshot is time in milliseconds with *time 0* denoting the onset of pacing. Note rate-dependent conduction slowing after heptanol on the snapshots and on the isochronal maps.

continuously acquired using Axoscope software, a Digidata acquisition system (Axon Instruments) with a sampling interval of 200 μs and 14-bit resolution (14). The maximal voltage change over time (dV/dt_{max}) at PCLs of 400, 300, and 200 ms were measured from the digitized TMP data. Dynamic APD restitution curves (15) were then constructed during progressively shorter PCLs starting from 300 ms and decreasing by 10-ms increments (at PCL >190 ms) and by 2-ms increments (at PCL <80 ms) until block. The shortest 1:1 captured PCL was recorded before and after perfusion with 1–50 μM heptanol. The action potential duration (APD) repolarization to 90% (APD_{90}) against its previous diastolic interval was then plotted and fitted by a single exponential curve (Microcal, Origin 5.0).

Statistical analysis. All statistical analyses were performed using GB-STAT (7) Student's *t*-test for single comparison. ANOVA for multiple comparisons was used to compare the means. A Chi-square test was used to detect differences in the occurrence of sustained AF. The null hypothesis was rejected at a value of $P \leq 0.05$. Results are expressed as means ± SD.

RESULTS

Effect of heptanol on atrial capture rate. At 1 μM, heptanol had no effect on the fastest 1:1 captured atrial PCL (111 ± 2.3 ms). However, when heptanol concentration was >1 μM, a concentration-dependent loss of regular 1:1 atrial capture developed at significantly ($P < 0.01$) longer PCL. At baseline, the shortest regular 1:1 atrial captured PCL was 111 ± 2 ms, which increased to 127 ± 27, 146 ± 34, 168 ± 40, and 182 ± 46 ms during perfusion with 2, 5, 10, and 50 μM heptanol, respectively ($P < 0.01$ for all comparisons). The effects of heptanol were reversible. Within 30 min of drug-free Tyrode perfusion, the atria could be captured at the same pre-heptanol shortest CLs (113 ± 2.8 vs. 111 ± 2.3 ms, P = not significant).

Effects of heptanol on CV. Heptanol at 2 μM but not at 1 μM caused significant ($P < 0.001$) CV slowing along the fiber at all three (600, 400, and 200 ms) PCLs tested. At baseline, the CV at these three PCLs were 64.2 ± 2.7, 53.8 ± 4.7, and 38.5 ± 4.5 cm/s, respectively, and decreased to 38.8 ± 0.9, 29.9 ± 3.3, 23.1 ± 2.4 cm/s, respectively, after heptanol ($P < 0.05$ for all comparisons). Figure 1 is a representative optical map showing conduction slowing after 2 μM heptanol perfusion at two different PCLs. At baseline, the wave front propagated with relative uniformity and without conduction slowing both at 400 and 130 ms PCL. However, after heptanol and during faster rates of pacing (CL < 200 ms), the CV became severely slowed and nonuniform (Fig. 1). When the CV was severely slowed, the propagation of the wave front became highly nonuniform, preventing its systematic and accurate measurement at pacing CLs <200 ms.

Induction of AF. At baseline, rapid pacing induced short runs of repetitive atrial activity that lasted 2.1 ± 1.5 s in 7 of 12 isolated atria (Fig. 2). No sustained AF (>30 s) could be induced at baseline in any of the 12 tissues studied. Perfusion with 1 μM heptanol did not change vulnerability to inducible AF. However, after 2 μM heptanol, sustained AF (>30 s) was induced in 9 of 12 tissues ($P < 0.001$). In 8 of 12 tissues, the induced AF lasted >5 min, requiring electrical shocks for termination. Shocks were applied through a pair of coil electrodes placed in the tissue bath at the edges of the

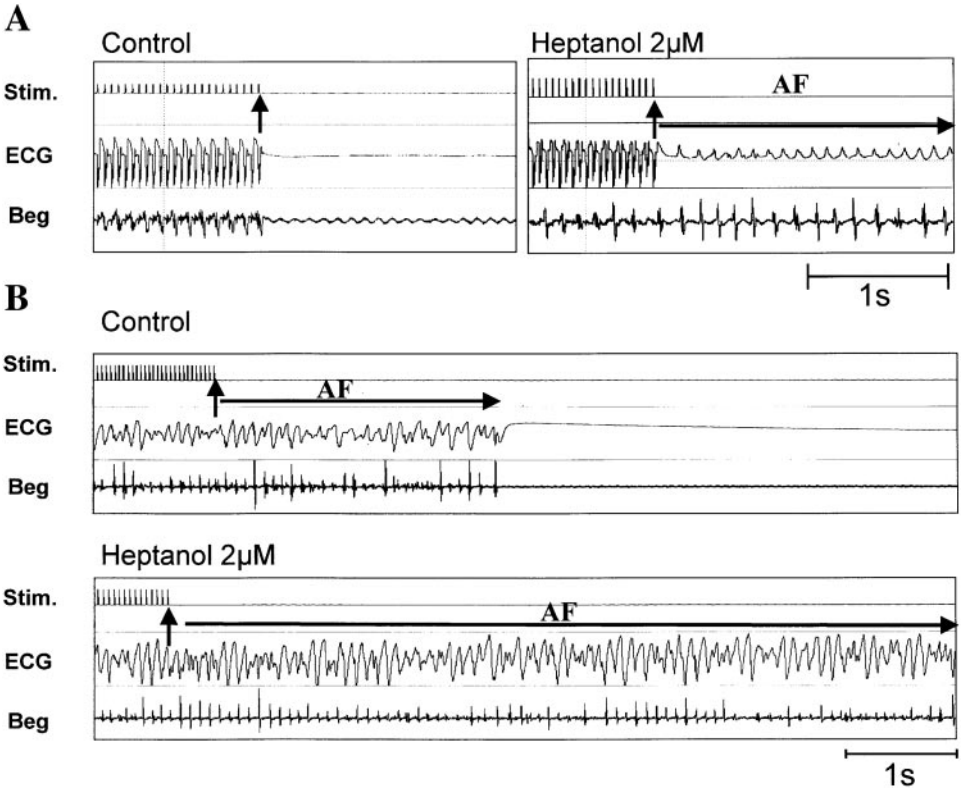

Fig. 2. Effects of heptanol on atrial rhythm during rapid atrial pacing. *A*: at baseline (control) no arrhythmia is induced. However, after 2 μM of heptanol, atrial fibrillation (AF) is induced. *B*: conversion of nonsustained AF (2.2 s) induced at baseline (control) to sustained AF after 2 μM heptanol. Stim, stimulus artifact; ECG, pseudoelectrocardiogram; BEg, bipolar atrial electrogram.

isolated tissues. Figure 2 illustrates examples of sustained AF induced after 2 μM heptanol and no arrhythmia or nonsustained AF induced at baseline. In addition to sustained AF, nonsustained AF lasting on the average for 7.2 ± 4.5 s ($P < 0.05$ compared with baseline) could also be induced in all 12 tissues after 2 μM heptanol perfusion.

Wave-front dynamics during induced AF. There were significant differences between the characteristics of AF induced at baseline and AF induced during heptanol perfusion. The CL of the induced AF was significantly shorter at baseline than after 2 μM heptanol perfusion (114 ± 8 vs. 128 ± 12 ms for AF CL, $P < 0.01$). The AF, at baseline and during heptanol perfusion, was characterized by the presence of multiple independent wave fronts with a characteristic fibrillation-like electrogram both on the pseudoelectrocardiogram and the local atrial electrogram (Fig. 2). The AF was maintained by continuous wave-front breakups, providing a source of multiple independent wave fronts. The average number of independent wave fronts (i.e., number of wave fronts propagating in different directions per second in the optical field of view) during AF was significantly ($P < 0.01$) smaller at baseline (1.6 ± 0.3) than after heptanol (2.2 ± 0.4). In 26 episodes of heptanol-induced sustained AF, 69 events of spontaneous wavebreaks were captured and analyzed. Of these 69 events, 46 episodes of wave breaks developed across and 23 along the fiber. Block across the fiber developed at significantly longer coupling intervals (i.e., the interval between the previous activation and the activation causing wave break) than those along the fiber orientation (102 ± 24 vs. 74 ± 15 ms; $P < 0.001$). During the induced AF, the incidence of wave breaks in the optical field of view was significantly higher in the presence of heptanol than at baseline (3.8 ± 1.6 vs. 6.3 ± 2.1 s^{-1}, respectively, $P < 0.001$). During the induced AF, the average CV of the wavelets was significantly ($P < 0.01$) faster at baseline than during 2 μM heptanol perfusion (27.3 ± 8.6 vs. 19.3 ± 10.2 cm/s, respectively).

Mechanism of heptanol-induced AF: conduction block and reentry. Figure 3 illustrates activation pattern at baseline during 2:1 atrial capture at a stimulating CL of 50 ms CL (i.e., captured CL = 100 ms). At baseline, the wave front propagated with a relatively uniform pattern without block during the entire pacing sequence (only the first two beats are shown). However, after 2 μM heptanol, at 50 ms CL of stimulation, the first captured wave front propagated slowly and in a nonuniform fashion. During the second captured beat at a CL of 100 ms, the wave front underwent conduction block across the fiber (Fig. 3). Block was then followed by a clockwise rotation of the wave front at a CL of 75 ms. The block was functional because propagation proceeded without block at baseline (Fig. 3*A*). During the second rotation, another wave front entered the mapped region from the bottom, signaling the onset of AF (Fig. 3). Induction of AF with heptanol was highly concentration dependent. Raising heptanol concentration to 5 μM and higher (up to 50 μM) caused loss of rapid atrial capture and inability to induce AF.

Effects of heptanol on TMP and APD restitution. In three dogs, we recorded TMP before and after 2 μM heptanol. There was no significant difference in the dV/dt_{max} at PCL of 400, 300, and 200 ms. At baseline, the dV/dt_{max} were 40.8 ± 4.1, 33.4 ± 2.8, and 31.5 ± 2.3 V/s, respectively. After 2 μM heptanol perfusion the dV/dt_{max} at these three PCLs were 37.9 ± 3.6, 33.4 ± 2.8, and 29.6 ± 2.1 V/s, respectively (P = not significant for all comparisons) (Fig. 4). Heptanol (2 μM) had no significant effect on the APD at all pacing CLs studied (400–200 ms) and no maximum slope of the dynamic APD restitution curve in all three tissues (0.85 ± 0.08 vs. 0.80 ± 0.14; P = not significant) (Fig. 4).

DISCUSSION

Major findings. The ability of partial cellular uncoupling with heptanol to increase the incidence and duration of inducible AF in normal canine atria without changing the active cellular properties constitutes the major finding of this study. Critical uncoupling (2 μM) seemed to be necessary for increased vulnerability to inducible AF. Heptanol at 1 μM, 5 μM, and higher failed to promote inducible AF.

Mechanisms of heptanol-induced AF. Heptanol-induced AF was preceded by nonuniform atrial conduction slowing that eventually underwent block with subsequent formation of reentry leading to AF. The ability of heptanol to cause nonuniform atrial conduction slowing is consistent with previous experimental (28) and simulation (16, 27) studies. For example, Jalife et al. (11) have shown that low concentrations of heptanol cause significant ventricular conduction slowing with no or only minimal changes in the fast sodium current and action potential properties. These findings in the ventricular myocardium are consistent with the present data in atrial tissue. Simulation studies have shown that decreased cellular coupling (i.e., increased gap junctional resistance) unmasks dispersion of APD, a phenomenon that leads to increased spatial dispersion of excitability (16, 27). Because heptanol increases gap junctional resistance (25), it is possible that the nonuniformity of wave-front propagation seen in the present study could have resulted from increased spatial dispersion of atrial excitability (6).

Conduction slowing and block. Heptanol-induced conduction slowing, conduction block, and reentry appear to be independent of the potential influence of heptanol on the active cellular properties of the atrium (20, 25). This suggestion is supported by the following two findings. First, the concentration of heptanol (2 μM) that promoted inducible AF was not associated with any significant effect on the dV/dt_{max} of the action potential upstroke, indicating that the observed wave break was independent of the potential of heptanol to block sodium ion channels (20). Second, heptanol at 2 μM did not change the slope of the dynamic APD restitution curve or atrial APD, indicating that the mechanism of heptanol for increasing AF vulnerability

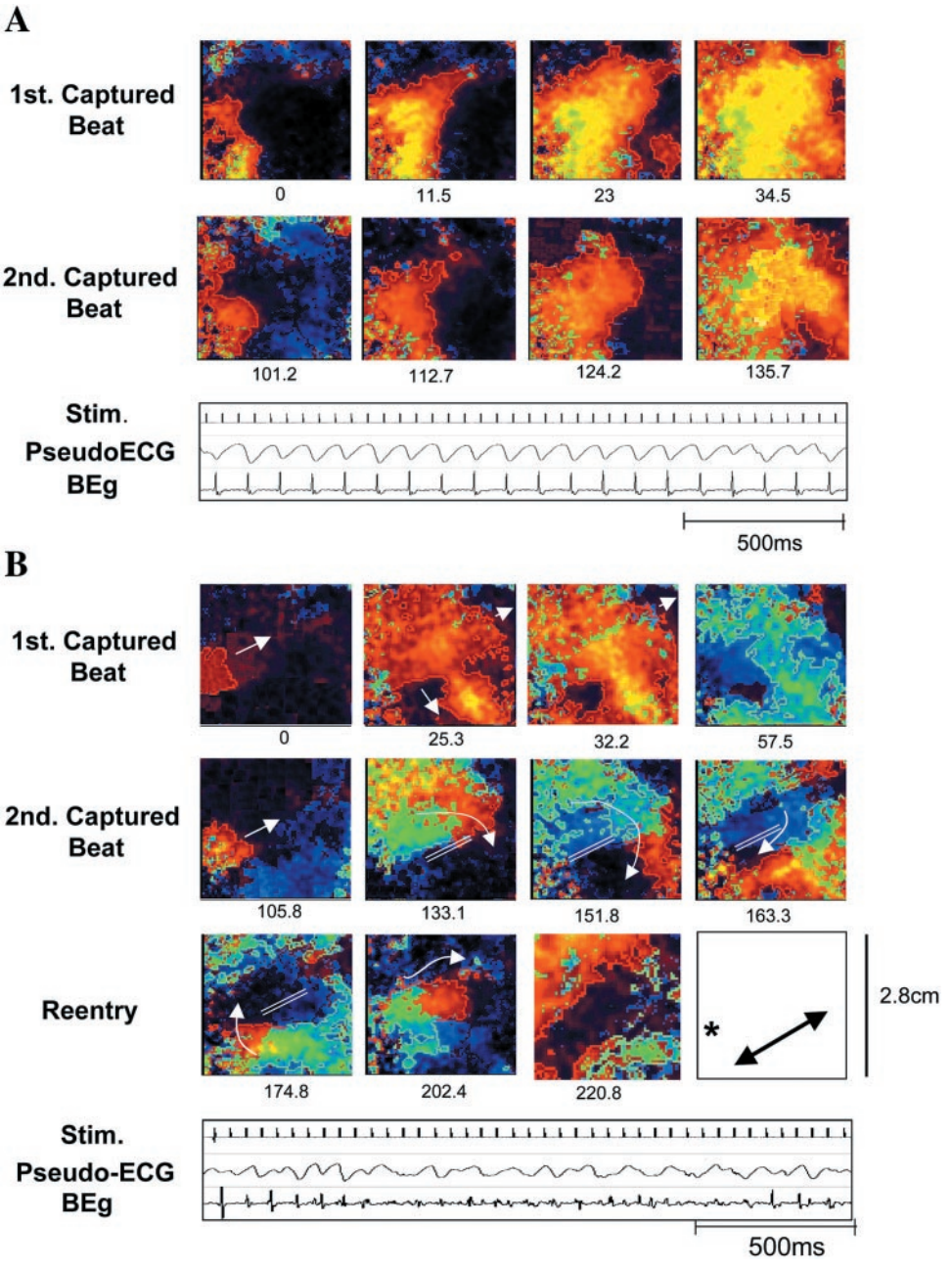

Fig. 3. Induction of reentry during rapid atrial pacing in a canine left atrium exposed to 2 μM heptanol. *A*: baseline (control) showing 2:1 capture during pacing at 50-ms PCL with regular and relatively uniform propagation after each paced beat. However, after 2 μM heptanol (*B*), the first captured beat propagates slowly and nonuniformly (arrows), whereas the second captured beat undergoes functional conduction block (double lines). Block then leads to the formation of a clockwise reentrant activation (arrows). After the completion of the first rotation at a cycle length of 72 ms (snapshots 133.1 ms and 202.4 ms), another wave front enters the mapped region from the lower right part of the mapped field, signaling the onset of AF. Abbreviations are as in Fig. 1. The last frame shows the pacing site (*) and the fiber orientation (double-headed arrow).

is not mediated to the APD restitution hypothesis (29). In line with the cellular uncoupling hypothesis of atrial vulnerability to tachyarrhythmias is the demonstration of atrial conduction disturbances and rapid atrial pacing-induced atrial tachyarrhythmias in transgenic mice with Cx40 deficiency (8).

Heptanol and the mechanism of AF maintenance. During AF, frequent wave breaks developed both across and along the fiber. Wave breaks developed more frequently across than along the fiber (67% vs. 33%). The recovery period at the site of the wave break along and across the fiber was significantly shorter than the mean AF CL. Whereas a temporal excitable gap is known to exist during AF (10, 30), early premature wave fronts may block as they encroach the refractory tail of the previous waves (i.e., outside the excitable gap). In the present study it is possible that the wave fronts that blocked along the fiber at coupling intervals of ~58% of the mean AF CL may have resulted from the residual refractoriness left behind by the previous wave front. In contrast, block across the fiber developing at coupling intervals longer or equal to 80% of the AF CL suggests, but does not prove, that block across the fiber can result from a heptanol-induced increase in side-to-side gap junctional resistance (24). Wave breaks were often followed by the formation of a reentrant wave front of excitation that could be sustained for a short period (atrial flutter), or underwent breakup, leading to multiple and irregular wavelets characteristic of AF (9, 31).

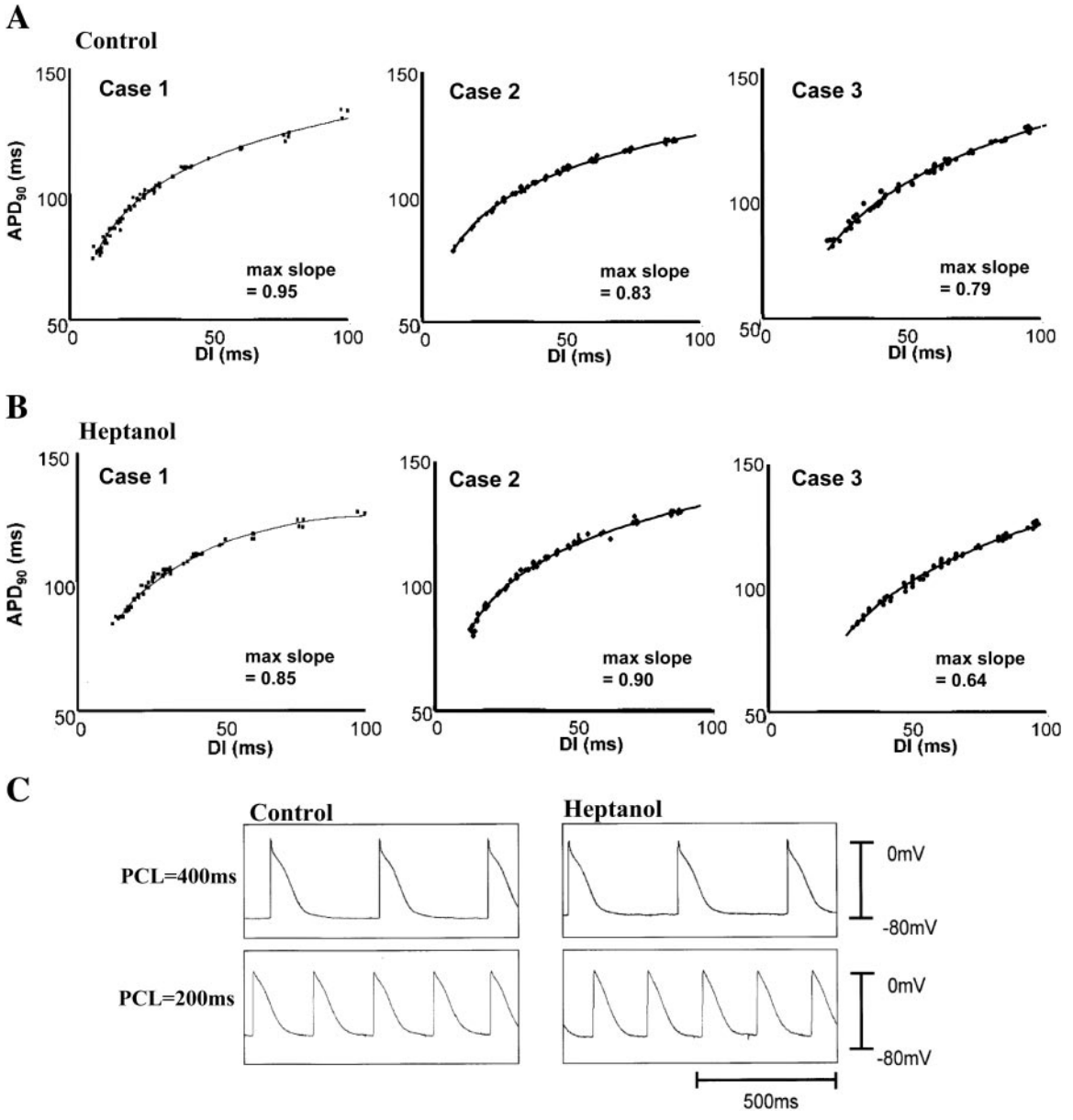

Fig. 4. Dynamic transmembrane action potential duration (APD) restitution curves to 90% repolarization (APD_{90}) before (*A*) and after (*B*) 2 μM heptanol in three atrial tissues (*cases 1–3*). Note that the maximum (max) slope of the APD_{90} remains <1 after heptanol. *C*: atrial transmembrane action potential recordings during 400- and 200-ms PCL before (control) and during 2 μM heptanol perfusion. Heptanol produces no detectable effect on either APD restitution curves in all three tissues or transmembrane action potential properties. DI is diastolic interval.

Limitation of the study. It may be argued that two-dimensional mapping of a three-dimensionable structure may miss important insights. However, our ability to demonstrate heptanol-induced wave break during rapid pacing leading to reentry and subsequent breakups, causing sustained AF, allowed us to effectively test the partial cellular uncoupling hypothesis of increased vulnerability to inducible AF in the canine atria.

Clinical implications. Atrial remodeling causing enhanced AF vulnerability engages either transmembrane ionic changes (electrical remodeling) (6, 32) or atrial structural changes, including interstitial atrial fibrosis (anatomic remodeling) (1, 17). Remodeling of the gap junctions that may result from cardiac adaptive processes (23) or from cardiac diseases (21) may also lead to enhanced AF vulnerability.

In conclusion, during rapid pacing, critically low concentrations of heptanol cause conduction slowing, wavebreak, and reentry leading to AF. The heptanol-induced increase in AF vulnerability may be mediated by partial cellular uncoupling (increased gap junctional resistance) because transmembrane action potential upstroke and APD restitution remain unchanged after heptanol.

We thank Avile McCullen and Yasushi Miyauchi for technical assistance, Elaine Lebowitz for secretarial assistance, Nina Wang for reading the manuscript, and Drs. C. T. Peter, Teruo Takano, and P. K. Shah for their support.

This study was supported in part by National Heart, Lung, and Blood Institute Specialized Center of Research Grant HL-52319, the Cedars-Sinai ECHO Foundation and Grand Sweepstakes, American Heart Association (AHA) National Center Grant-in-Aid 9750623N and 9956464N, AHA Scientist Development Award 0130171N, Fukuda Foundation for Medical Technology, University of California Tobacco-Related Disease Research Program (9RT-0041), and the Pauline and Harold Price Endowment.

REFERENCES

1. **Ausma J, Wijffels M, Thone F, Wouters L, Allessie M, and Borgers M.** Structural changes of atrial myocardium due to sustained atrial fibrillation in the goat. *Circulation* 96: 3157–3163, 1997.
2. **Balke CW, Lesh MD, Spear JF, Kadish A, Levine JH, and Moore EN.** Effects of cellular uncoupling on conduction in anisotropic canine ventricular myocardium. *Circ Res* 63: 879–892, 1988.
3. **Benjamin EJ, Levy D, Vaziri SM, D'Agostino RB, Belanger AJ, and Wolf PA.** Independent risk factors for atrial fibrillation in a population-based cohort: The Framingham Heart Study. *JAMA* 271: 840–844, 1994.
4. **Brugada J, Mont L, Boersma L, Kirchlof C, and Allessie MA.** Differnetial effects of heptanol, potassium, and tetrodotoxin on reentrant ventricular tachycardia around a fixed obstacle in anisotropic myocardium. *Circulation* 84: 1307–1318, 1991.
5. **Cao JM, Qu Z, Kim YH, Wu TJ, Garfinkel A, Weiss JN, Karagueuzian HS, and Chen PS.** Spatiotemporal heterogeneity in the induction of ventricular fibrillation by rapid pacing: importance of cardiac restitution properties. *Circ Res* 84: 1318–1331, 1999.
6. **Fareh S, Villemaire C, and Nattel S.** Importance of refractoriness heterogeneity in the enhanced vulnerability to atrial fibrillation induction caused by tachycardia-induced atrial electrical remodeling. *Circulation* 98: 2202–2209, 1998.
7. **Friedman P.** *GBStat*. Silver Spring, MD: Dynamic Microsystems, 1995.
8. **Hagendorff A, Schumacher B, Kirchhoff S, Luderitz B, and Willecke K.** Conduction disturbances and increased atrial vulnerability in Connexin40-deficient mice analyzed by transesophageal stimulation. *Circulation* 99: 1508–1515, 1999.
9. **Ikeda T, Wu TJ, Uchida T, Hough D, Fishbein MC, Mandel WJ, Chen PS, and Karagueuzian HS.** Meandering and unstable reentrant wave fronts induced by acetylcholine in isolated canine right atrium. *Am J Physiol Heart Circ Physiol* 273: H356–H370, 1997.
10. **Ikeda T, Yashima M, Uchida T, Hough D, Fishbein MC, Mandel WJ, Chen PS, and Karagueuzian HS.** Attachment of meandering reentrant wave fronts to anatomic obstacles in the atrium. Role of the obstacle size. *Circ Res* 81: 753–764, 1997.
11. **Jalife J, Sicouri S, Delmar M, and Michaels DC.** Electrical uncoupling and impulse propagation in isolated sheep Purkinje fibers. *Am J Physiol Heart Circ Physiol* 257: H179–H189, 1989.
12. **Joyner RW.** Mechanisms of unidirectional block in cardiac tissues. *Biophys J* 35: 113–125, 1981.
13. **Joyner RW.** Effects of the discrete pattern of electrical coupling on propagation through an electrical syncytium. *Circ Res* 50: 192–200, 1982.
14. **Kim YH, Yashima M, Wu TJ, Doshi R, Chen PS, and Karagueuzian HS.** Mechanism of procainamide-induced prevention of spontaneous wave break during ventricular fibrillation. Insight into the maintenance of fibrillation wave fronts. *Circulation* 100: 666–674, 1999.
15. **Koller ML, Riccio ML, and Gilmour RF Jr.** Dynamic restitution of action potential duration during electrical alternans and ventricular fibrillation. *Am J Physiol Heart Circ Physiol* 275: H1635–H1642, 1998.
16. **Lesh MD, Pring M, and Spear JF.** Cellular uncoupling can unmask dispersion of action potential duration in ventricular myocardium. A computer modeling study. *Circ Res* 65: 1426–1440, 1989.
17. **Li D, Fareh S, Leung TK, and Nattel S.** Promotion of atrial fibrillation by heart failure in dogs: atrial remodeling of a different sort. *Circulation* 100: 87–95, 1999.
18. **Lin SF, Roth BJ, and Wikswo JP Jr.** Quatrefoil reentry in myocardium: an optical imaging study of the induction mechanism. *J Cardiovasc Electrophysiol* 10: 574–586, 1999.
19. **Lin SF and Wikswo JP Jr.** Panoramic optical imaging of electrical propagation in isolated heart. *J Biomed Opt* 4: 200–207, 1999.
20. **Nelson WL and Makielski JC.** Block of sodium current by heptanol in voltage-clamped canine cardiac Purkinje cells. *Circ Res* 68: 977–983, 1991.
21. **Peters NS and Wit AL.** Myocardial architecture and ventricular arrhythmogenesis. *Circulation* 97: 1746–1754, 1998.
22. **Rudy Y and Quan WL.** A model study of the effects of the discrete cellular structure on electrical propagation in cardiac tissue. *Circ Res* 61: 815–823, 1987.
23. **Spach MS.** Changes in the topology of gap junctions as an adaptive structural response of the myocardium. *Circulation* 90: 1103–1106, 1994.
24. **Spach MS and Dolber PC.** Relating extracellular potentials and their derivatives to anisotropic propagation at a microscopic level in human cardiac muscle. Evidence for electrical uncoupling of side-to-side fiber connections with increasing age. *Circ Res* 58: 356–371, 1986.
25. **Takens-Kwak BR, Jongsma HJ, Rook MB, and Van Ginneken AC.** Mechanism of heptanol-induced uncoupling of cardiac gap junctions: a perforated patch-clamp study. *Am J Physiol Cell Physiol* 262: C1531–C1538, 1992.
26. **Valderrábano M, Kim YH, Yashima M, Wu TJ, Karagueuzian HS, and Chen PS.** Obstacle-induced transition from ventricular fibrillation to tachycardia in isolated swine right ventricles: insights into the transition dynamics and implications for the critical mass. *J Am Coll Cardiol* 36: 2000–2008, 2000.
27. **Viswanathan PC, Shaw RM, and Rudy Y.** Effects of IKr and IKs heterogeneity on action potential duration and its rate dependence: a simulation study. *Circulation* 99: 2466–2474, 1999.
28. **Weiss JN, Chen PS, Qu Z, Karagueuzian HS, and Garfinkel A.** Ventricular fibrillation: how do we stop the waves from breaking? *Circ Res* 87: 1103–1107, 2001.
29. **Weiss JN, Garfinkel A, Karagueuzian HS, Qu Z, and Chen PS.** Chaos and the transition to ventricular fibrillation: a new approach to antiarrhythmic drug evaluation. *Circulation* 99: 2819–2826, 1999.
30. **Wijffels MC, Dorland R, Mast F, and Allessie MA.** Widening of the excitable gap during pharmacological cardioversion of atrial fibrillation in the goat: effects of cibenzoline, hydroquinidine, flecainide, and D-sotalol. *Circulation* 102: 260–267, 2000.
31. **Wu TJ, Yashima M, Xie F, Athill CA, Kim YH, Fishbein MC, Qu Z, Garfinkel A, Weiss JN, Karagueuzian HS, and Chen PS.** Role of pectinate muscle bundles in the generation and maintenance of intra-atrial reentry: potential implications for the mechanism of conversion between atrial fibrillation and atrial flutter. *Circ Res* 83: 448–462, 1998.
32. **Yue L, Feng J, Gaspo R, Li GR, Wang Z, and Nattel S.** Ionic remodeling underlying action potential changes in a canine model of atrial fibrillation. *Circ Res* 81: 512–525, 1997.